Photochemical Formation of Copper(I) from Copper(II)-Dicarboxylate Complexes: Effects of Outer-Sphere versus Inner-Sphere Coordination and of Quenching by Malonate

Chien-Hou Wu,* Lizhong Sun,† and Bruce C. Faust‡

University of California at Los Angeles, Department of Civil and Environmental Engineering, Environmental Chemistry Laboratory, 5731 Boelter Hall, Los Angeles, California 90095-5731

Received: July 29, 1999; In Final Form: March 14, 2000

Copper(I) quantum yields are reported for Cu(II) complexes of aliphatic dicarboxylates in aqueous solution (N_2-purged), based on steady-state illuminations. For Cu(dicarboxylate)^0, the Cu(I) quantum yields at 313 nm ($\Phi_{Cu(I),CuL}$) exhibit the following trend (25 °C, ionic strength = 0.10 M): malonate (0.15 ± 0.07) > succinate (0.10 ± 0.02) (Sun, L.; Wu, C.-H.; Faust, B. C. *J. Phys. Chem. A* **1998**, *102*, 8664−8672) > glutarate (0.054 ± 0.005) > adipate (0.042 ± 0.004) ≈ pimelate (0.046 ± 0.009). The systematic decrease in Cu(I) quantum yield observed for these Cu(dicarboxylate)^0 complexes parallels the increasing degree of outer-sphere coordination of the complexes. Free uncomplexed malonate species quench the photoformation of Cu(I) from Cu(malonate)^0 in a way that cannot be explained solely based on the Cu(II) speciation. An interpretation based on the quenching of the intermediate [Cu($^{\cdot}CH_2C(O)O^-$)^0] by H(malonate)$^-$/H_2(malonate)^0 is proposed. Evidence is presented for Cu(I) photoformation from Cu(malonate)^0.

Introduction

The chemical speciation of Cu(II) plays an important role in controlling the bioavailability and the toxicity of copper to phytoplankton and other organisms in marine and freshwater environments.[1−3] In natural waters, Cu(II) is primarily present as complexes with natural and biogenic organic ligands.[4−9] Based on previous studies, Cu(II) complexes of organic ligands are significantly photoreactive at terrestrial solar wavelengths >290 nm.[10−13] Therefore, photochemical reactions of Cu(II) complexes can affect the redox cycling of copper, and hence the speciation of copper, and its bioavailability/toxicity to phytoplankton and other organisms in natural waters.

Photochemical reactions of Cu(II) complexes of a series of structurally related dicarboxylate ligands are of interest because they are representative of the coordination environment of organically bound Cu(II) in marine and freshwater environments.[14,15] Our previous study focused on the photoformation of Cu(I) from a series of structurally related inner-sphere Cu(II) complexes.[16] The Cu(I) quantum yields of Cu(dicarboxylate)^0 vary by a factor of 50 for the following inner-sphere Cu(II) complexes: oxalate (0.42), succinate (0.10), and maleate (0.008). The trend in Cu(I) quantum yields follows the order expected in terms of resonance stability of the carbon-centered radicals.

The previous study mainly dealt with Cu(II)/dicarboxylate complexes that exhibit primarily inner-sphere type coordination. For the Cu(II)/malonate system, the photoformation of Cu(I) showed a unique behavior which could not be quantitatively interpreted using the model in the previous study. Although there is qualitative information about the reaction pathway, a quantitative assessment of the mechanistic aspects of this process is lacking.[17] Therefore, this work explored the effect of outer-sphere versus inner-sphere coordination on the Cu(I) quantum yields of structurally related Cu(II)/dicarboxylates and characterized the quantum yield and mechanism of Cu(I) photoformation from Cu(malonate)^0.

Experimental Section

Materials and Solution Preparation. Except where noted, all chemicals were of the same purity and from the same sources as described previously.[16] All of the ligands were obtained from Fluka (heavy metal impurities <0.0005% m/m): malonic acid (>99%); glutaric acid (>98%); adipic acid (>99%); pimelic acid (>99%). All solutions were prepared using only ultrahigh-purity Milli-Q water (≥18.2 MΩ-cm resistivity). Solutions (or aliquots) were filtered through a 0.2 μm syringe filter (13 mm Teflon, or 25 mm Tuffryn; Acrodisc, Gelman). Gastight injection vials (40 mL, 28 × 95 mm, ≈ 22-mm Teflon-faced silicone septa, National Scientific Co.) were used to N_2-purge stock solutions of bathocuproine, Cu(I), and Cu(II). Glassware and quartzware were cleaned using a 50/50 v/v mixture of methanol (99.9%, Fisher, spectranalyzed) and aqueous 3.0 M HCl (Mallinckrodt), and thoroughly rinsed with Milli-Q water.[18]

Table 1 summarizes the solution conditions used for this study, which were optimized from the equilibrium speciation calculations. Typically, total initial concentration of Cu(II) ($[Cu(II)]_T$) and total initial concentration of dicarboxylate ligand ($[L]_T$) were held constant while pH was varied, or pH and $[Cu(II)]_T$ were kept constant while $[L]_T$ was varied. The criteria of a minimum absorbance of ≈ 0.010 (at 313 nm) due solely to Cu(II) species almost always limited the lowest total Cu(II) concentration that could be used for photochemical experiments.

Analytical Equipment and Measurements. Ultraviolet−visible absorbance measurements were made with a Varian Cary 3E UV/Vis spectrophotometer and a custom-built constant-temperature (25 °C, Fisher 910 recirculator) variable-path-length aluminum cuvette holder (black-anodized). Absorbance measurements of Cu(II) solutions were carried out in Teflon-

* To whom correspondence may be addressed: Beckman Institute (139-74), Division of Chemistry and Chemical Engineering, California Institute of Technology, Pasadena, CA 91125. E-mail: wu@peer.caltech.edu.

† Present address: Applied Materials, 3111 Coronado Drive, M/S 1512, Santa Clara, CA 95054.

‡ Present address: 11937 Kiowa Ave. Apt. 9, Los Angeles, CA 90049.

10.1021/jp992665x CCC: $19.00
Published on Web 04/29/2000

TABLE 1: Composition of Cu(II)/Dicarboxylate Solutions[a]

dicarboxylate (L)	$[Cu(II)]_T$ μM	$[L]_T$ μM	pH
malonate	50	5000	4.00−7.00
	50	400−5000	7.00
	50	500	5.00−7.00
	50	25, 2000	6.00
	60	500, 2000	7.00
glutarate	50	50 000	4.25−6.00
	50	5000−30 000	6.00
adipate	50	50 000	4.50−6.00
	50	7000−35 000	6.00
pimelate	50	3000	4.00−6.00
	50	3000−21 000	6.00

[a] All solutions were studied at 25 °C, they contained 100 μM total orthophosphate to buffer the pH (± 0.03), they had an ionic strength of 0.10 M (adjusted with NaCl, almost always 0.10 M), and they were filtered (0.2 μm). All solutions for photochemical experiments and Cu(I) measurements were N_2-purged. All solutions for spectral measurements were saturated with ambient laboratory air. Solutions did not contain any precipitates, and were below the calculated solubility limit of all solids. $[Cu(II)]_T$ = total concentration of Cu(II). $[L]_T$ equals the total concentration of dicarboxylate ligand. The exact composition of each solution studied is described in the Supporting Information.

stoppered 10.00-cm quartz cuvettes (Starna). Photochemical experiments and chemical actinometry were done in gastight 100% fused-quartz cuvettes (5.00 cm path length, Spectrocell Inc.; R-3050-I; FUV; modified to 70 mm overall height) equipped with a 12-mm Teflon-faced silicone septum (Sun Brokers, 200594) and a Teflon screw cap. Solution pH was measured with an Orion Model SA 720 pH meter and combination glass electrode (Orion 8103 Ross). The pH measurements were calibrated with NIST-traceable standard buffers (Fisher).

Copper(I) was quantitatively determined using the bathocuproine method.[19,20] N_2-purging was used to remove O_2 from solutions of Cu(II)/dicarboxylate, bathocuproine, Cu(I), and Cu(II) to ensure an accurate measurement of Cu(I).[16] The apparent first-order rate constant for direct photoproduction of Cu(I) from a given Cu(II)/dicarboxylate complex (CuL and CuL_2) in terrestrial sunlight ($j_{i\rightarrow Cu(I)}$) was estimated by using procedures described in refs 21 and 22. Values of the volume-averaged incident irradiance I_0 (einstein L^{-1} s^{-1}) at 313 nm were determined by 2-nitrobenzaldehyde chemical actinometery.[23]

The activity of Cu^{2+} in solution was measured using an Orion Model SA 720 pH meter, an Orion 9429 Cu^{2+} ion selective electrode, a 90-02 double junction reference electrode, and Cu^{2+} activity standards (log $\{Cu^{2+}\} = -6.74$ to -3.44) prepared by volumetric dilution. The electrode response stabilized within 1 min at total copper concentrations above 10^{-5} M. Cu(II)/malonate solutions for Cu^{2+} activity measurements were prepared by the same procedure, but with $Cu(NO_3)_2$ and $NaNO_3$ (instead of $CuCl_2$ and NaCl) to avoid Cl^- interferences in potentiometry.[24]

Photoproducts were detected using a Waters 510 HPLC and an ABI 783 absorbance detector (215 nm) with a Corogel 64H ion exclusion column (300 × 7.8 mm ID) and 87H guard column (InterAction Chromatography) using 5.0 mM H_2SO_4 in 85%/15% v/v H_2O/CH_3CN as the mobile phase (0.6 mL/min), maintained at 42 °C (Eppendorf CH-30 column heater, TC-50 temperature control). Acetate and glycolate standards were gravimetrically prepared.

Results and Discussion

Copper(II) Speciation. The equilibrium Cu(II) speciation (25 °C) was calculated for each Cu(II)/dicarboxylate system studied, using the MINTEQA2 computer program with equilibrium constants of major Cu(II)/dicarboxylates listed in Table 2, the known solution composition ($[Cu(II)]_T$, $[L]_T$, pH, 100 μM total orthophosphate), and ionic strength (0.10−0.20 M NaCl).[25−28] As described previously,[16] the lowest possible Cu(II) concentration was used to avoid any possible formation of Cu(II)/dicarboxylate dimers. The highest Cu(II) concentration used in the study was 60 μM, which is lower than the concentration (500 μM) at which Fe(III) is known to form polymeric species; Cu(II) is less prone to forming polymeric species than is Fe(III).[29]

From the equilibrium speciation calculation for the conditions of the photochemical experiments, the complexes CuL, CuL_2, and Cu(HL) represented cumulatively the following percentage of the total Cu(II) species [$100(f_{CuL} + f_{CuL2} + f_{Cu(HL)})$ where f_i is the equilibrium fraction of the total copper present as the ith complex]: ≥36% for malonate, ≥48% for glutarate, ≥52% for adipate, and ≥27% for pimelate. For the 313-nm spectral measurements done at pH <7.00, the complexes CuL, CuL_2, and Cu(HL) represented cumulatively the following percentages of the total Cu(II) species [$100(f_{CuL} + f_{CuL2} + f_{Cu(HL)})$]: ≥95% for malonate, ≥48% for glutarate, ≥58% for adipate, and between 0 and 27% for pimelate. Under the conditions of this study, the fraction of all forms of inorganic Cu(II) species (f_{in}) was not negligible; nevertheless, the absorbance of these species is weak and their photolysis inefficient, even compared to the least reactive Cu(II)/dicarboxylate complex studied here. All Cu(II)/dicarboxylate solutions studied here were calculated to be undersaturated with respect to all possible solid phases (e.g., CuO(s), $CuCO_3$(s), $Cu_3(PO_4)_2$, etc.) which may occur in the experimental solutions. Also, solid phases were not visible or detectable over the experimental timescale.

To confirm the speciation calculation for the Cu(II)/malonate system, the Cu^{2+} activity, $\{Cu^{2+}\}$, was measured by potentiometry for Cu(II)/malonate solutions identical to those used for experiments except that nitrate salts were used instead of chloride salts to avoid Cl^- interferences. Figure 1 shows that the measured Cu^{2+} activity, $\{Cu^{2+}\}$, was in good agreement (within 10%) with $\{Cu^{2+}\}$ values from the equilibrium speciation calculations.

Molar Absorptivities of Individual Cu(II) Complexes. Molar absorptivities (ϵ_i, M^{-1} cm^{-1}) at a given wavelength for individual species were determined as

$$\epsilon_{Cu(II)} = \sum_i \epsilon_i f_i \qquad (1)$$

where $\epsilon_{Cu(II)}$ is the experimental Cu(II)-based molar absorptivity, ϵ_i is the fundamental molar absorptivity of individual Cu(II) complexes, and f_i is the equilibrium fraction of the total copper present as the ith complex.[30] Equation 1 indicates that the observed value, $\epsilon_{Cu(II)}$ is a linear combination of the weighted molar absorptivities of individual Cu(II) species. Therefore, the fundamental molar absorptivities of individual Cu(II) complexes (e.g., ϵ_{CuL}, ϵ_{CuL_2}) can be determined from a multivariate linear regression of eq 1 by varying f_i.

Table 3 shows the values of molar absorptivities of individual complexes (CuL) at 313 nm for each Cu(II)/dicarboxylate system studied here. The experimental data demonstrate that Cu(II)/glutarate, Cu(II)/adipate, and Cu(II)/pimelate complexes, which share a similar transition between Cu(II) and ligands, have very comparable molar absorptivities at 313 nm.

Kinetics of Cu(I) Photoproduction from Cu(II)/Dicarboxylates. Earlier studies have established that for an aqueous Cu(II) solution with low total absorbance (A ≤0.12), and where

TABLE 2: Composition Matrix for the Calculated Equilibrium Speciation of Cu(II): Cu(II) Species, and their Corresponding Components, Stoichiometric Coefficients, and Equilibrium Formation Constants[a,b]

species	components[c] mal^{2-}	glu^{2}	$adip^{2-}$	pim^{2-}	Cu^{2+}	H^{+}	equilibrium constant[a] $\log(\beta)$	notes[d]
$Cu(mal)^0$	1				1		5.04	0.10, 25°
$Cu(Hmal)^+$	1				1	1	7.36	0.10, 25°
$Cu(mal)_2^{2-}$	2				1		7.80	0.10, 25°
$Cu(glu)^0$		1			1		2.37	0.10, 25°
$Cu(adip)^0$			1		1		2.3	0.10, 25°
$Cu(pim)^0$				1	1		2.21	0.10, 25°

[a] All equilibrium constants reported here are for 25 °C (except where noted otherwise), 1.0 atm, and ionic strength $I = 0.10$ M. In certain cases equilibrium constants have been converted from a value for another ionic strength to a value for ionic strength = 0.10 M (as listed in this table), using the Davies equation (ref 28). [b] Equilibrium formation constants (β) and pK_a values are from critical reviews (refs 26−27). [species] = β[component 1]^i[component 2]^j[component 3]^k . . ., where [ ] signifies molar concentration of the species/component; *i, j, k,* . . . are stoichiometric coefficients for the corresponding component (given in the matrix above), and β is the equilibrium formation constant of the species. Equilibrium constants for all inorganic Cu(II) species used here are identical to those given previously (ref 16). Blank entries in the table are zero. The pK_a values of the species (25 °C, 1.0 atm, $I = 0.10$ M; original source, and as used here) are: malonic acid (2.63, 5.28), glutaric acid (4.13, 5.01), adipic acid (4.27, 5.03), pimelic acid (4.31, 5.08), H_2CO_3* (6.13, 9.88) where $H_2CO_3^* \equiv H_2CO_3(aq) + CO_2(aq)$, and H_3PO_4 (1.92, 6.71, 11.65). For $K_w = [H^+][OH^-]$, $\log(K_w) = -13.78$ (25 °C, 1.0 atm, $I = 0.10$ M; original source, and as used here). [c] $mal^{2-} \equiv$ malonate^{2-}, $Glu^{2-} \equiv$ glutarate^{2-}, $adip^{2-} \equiv$ adipate^{2-}, and $pim^{2-} \equiv$ pimelate^{2-}. $Hmal^-$ represents the monoprotonated form of malonate. [d] Ionic strength (molar) and temperature (°C) of the original source of the thermodynamic data.

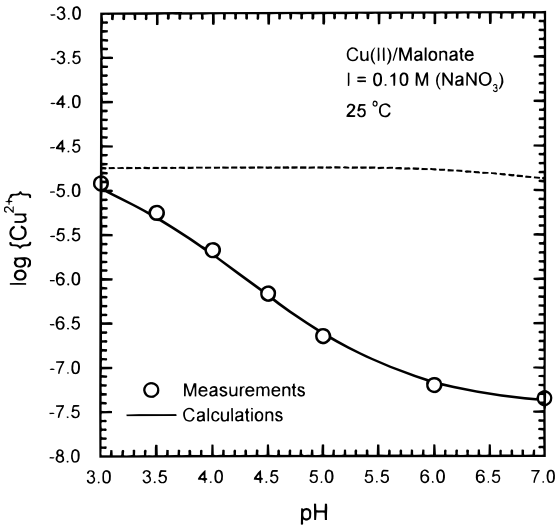

Figure 1. Comparison of the measured cupric ion activity, $\log\{Cu^{2+}\}$, and the calculated values. (○) Values of $\log\{Cu^{2+}\}$ measured for 50 μM total Cu(II), 2 mM malonate, 0.10 M sodium nitrate, and pH = 3.00 to 7.00 (Note that the potential response for the Cu−ISE was determined using dilute standards at 25 °C with $[Cu^{2+}] = 1.00 \times 10^{-3}$ to 5.00×10^{-7} M, 0.10 M sodium nitrate at pH 4). (—) Calculated values for conditions corresponding to experimental data. (- - -) Calculated values for inorganic complexation (without malonate) with otherwise identical composition.

the conversion of Cu(II) to Cu(I) is limited to <10% of the initial total Cu(II) concentration, the initial rate of Cu(I) photoproduction can be expressed in terms of experimental quantities as:[30]

$$R_{Cu(I)}{}^0 = 2.303 I_0 D \Phi_{Cu(I)} \epsilon_{Cu(II)} [Cu(II)]_T = j_{Cu(I)} [Cu(II)]_T \quad (2)$$

where I_0 is the volume-averaged incident irradiance (einstein L^{-1} s^{-1}), D is the optical path length (cm), and $\Phi_{Cu(I)}$ is the experimental Cu(I) quantum yield (mole einstein^{-1}). All of the parameters in the quantity $[R_{Cu(I)}{}^0/(2.303 I_0 D[Cu(II)]_T)]$ are measured or known. The initial rate method can provide the same kinetic information in the whole course of the reaction as long as the measurement is during this steady-state period that intermediates in the system reach their steady-state concentrations. Separate experiments have been performed to check this assumption in the Cu(II)/oxalate system ($[Cu(II)]_T = 10$ μM, pH = 5.00, $[L]_T = 500$ μM, 100 μM total orthophosphate, and 0.10M NaCl). The first-order rate is maintained over 3 half-lives in Cu(II)/oxalate system.

Figure 2 shows the results of Cu(I) photoproduction, which are typical for Cu(II)/dicarboxylate systems. Cu(I) photoproduction follows first-order kinetics characterized by an apparent first-order rate constant (s^{-1}). The first-order rate constant of Cu(I) photoproduction ($j_{Cu(I)}$) at 313 nm was determined from the linear-regression slope of the plot of $\ln\{[Cu(II)]_T/([Cu(II)]_T - [Cu(I)])\}$ versus illumination time.

Mechanisms and Cu(I) Quantum Yields with Model Ligands. Based on the results of previous studies and on the literature,[16,17,31−33] the photoredox process of Cu(II)/dicarboxylates can be depicted in Figure 3.

As shown in the figure, irradiation of Cu(II)/dicarboxylate complexes induces charge transfer and subsequent redox decomposition to Cu(I), CO_2, and various organic products. The photochemical transformation to Cu(I) involves several intermediates, some of which have been observed in flash photolysis.[31−34] These intermediates can be designated as a carboxylate radical (i.e., acyloxyl radical, carbonyloxyl radical, $^{\cdot}O(O)C-R-C(O)O^-$) and a carbon-centered radical ($^{\cdot}C-R-C(O)O^-$), both of which may be either free or bound in the water solvent cage with Cu(I). Since the Cu(I) quantum yield ($\Phi_{Cu(I)}$) is the ratio of total Cu(I) formed to photons absorbed, all contributions from direct and indirect photochemical reactions are incorporated into the reported Cu(I) quantum yield.

The photochemical reaction of Cu(II)-dicarboxylate complexes in Figure 3 can be represented by the following simplified mechanism. Note that, for simplicity, the proton-transfer reaction with water and the complexation reaction with the free ligand (present in excess) are not shown explicitly.

$$Cu(II)_i + h\nu \rightarrow\rightarrow\rightarrow [Cu(I)\text{-}{}^{\cdot}RC(O)O^-]_i + CO_2 \quad j_{i1} \quad (3)$$

$$[Cu(I)\text{-}{}^{\cdot}RC(O)O^-]_i \rightarrow Cu(I) + {}^{\cdot}RC(O)O^- \quad k_{i2} \quad (4)$$

$$[Cu(I)\text{-}{}^{\cdot}RC(O)O^-]_i + Q \rightarrow\rightarrow Cu(II)_i + HRC(O)O^- \quad k_{i3} \quad (5)$$

$$Cu(II)_i + {}^{\cdot}RC(O)O^- \rightarrow Cu(I) + R(OH)C(O)O^- \quad k_{i4} \quad (6)$$

where the subscript i represents the photochemical reaction

TABLE 3: Summary of Molar Absorptivities (ϵ_{CuL}, M^{-1} cm^{-1}) and Cu(I) Quantum Yields ($\Phi_{Cu(I),CuL}$, mol $einstein^{-1}$) for the Individual Cu(dicarboxylate)^0 (CuL) Complexes at 313 nm and a Comparison with the Fraction of Outer Sphere Coordination of Cu(dicarboxylate)^0 Complexes[a]

dicarboxylate $^-O(O)C-(CH_2)_n-C(O)O^-$	n	ϵ_{CuL}	$\Phi_{Cu(I),CuL}$	$(\Phi_{Cu(I),CuL})(\epsilon_{CuL})$	log(K)[b]	calculated contribution of outer sphere coordination[c]	source
oxalate	0	82 ± 23	0.42 ± 0.14	35 ± 6	4.85	0.0023	ref 16
malonate[d]	1	21 ± 4	0.15 ± 0.07	3.1 ± 1.2	5.04	0.0015	this work
succinate	2	70 ± 5	0.10 ± 0.02	7.1 ± 1.1	2.7	0.32	ref 16
glutarate	3	46 ± 2	0.054 ± 0.005	2.5 ± 0.2	2.37	0.69	this work
adipate	4	49 ± 4	0.042 ± 0.004	2.1 ± 0.1	2.3	0.79	this work
pimelate	5	51 ± 9	0.046 ± 0.009	2.3 ± 0.2	2.21	≈ 1	this work

[a] Mean value $\pm$ 1 standard deviation for 25 °C and 0.10 M ionic strength (NaCl). Solutions were purged with ultra-high purity N_2 for the Cu(I) quantum yield determinations. The range of solution compositions used to determine these values is given in Table 2 and in the Supporting Information. [b] $\beta = [Cu(dicarboxylate)^0]/([Cu^{2+}][dicarboxylate^{2-}])$ for 25 °C, ionic strength = 0.10 M (NaCl, almost always 0.10 M), 1 atm. [c] Estimated assuming that the β value for Cu(pimelate)^0 represents the approximate likely minimum value for outer sphere coordination of Cu(dicarboxylate)^0 for this series of complexes: contribution $= \beta_{pimelate}/\beta_{dicarboxylate}$. [d] $\epsilon_{CuL_2} = 30 \pm 4$ M^{-1} cm^{-1}. $\Phi_{Cu(I),CuL_2}\epsilon_{CuL_2} = 0.1 \pm 1.2$ L $einstein^{-1}$ cm^{-1}, and $k_{i3}/k_{i2} = (4.7 \pm 3.0) \times 10^4$ M^{-1}.

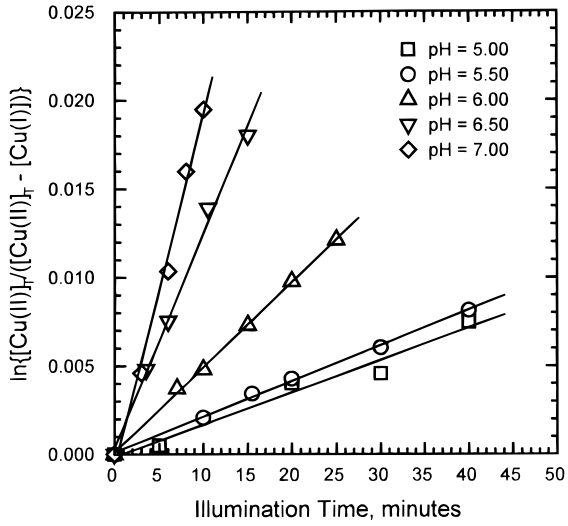

Figure 2. Kinetic behavior of Cu(I) photoproduction at 313 nm (25 °C) in the Cu(II)/malonate system with $[Cu(II)]_T = 50$ μM, $[malonate]_T = 500$ μM, pH = 5.00 to 7.00 (100 μM total orthophosphate), and ionic strength = 0.10 M NaCl. The slope of this plot (after correction for minor Cu(I) production in the dark) gives the apparent first-order photoreaction rate constant for Cu(I) photoproduction, $j_{Cu(I)}$ (eq 2).

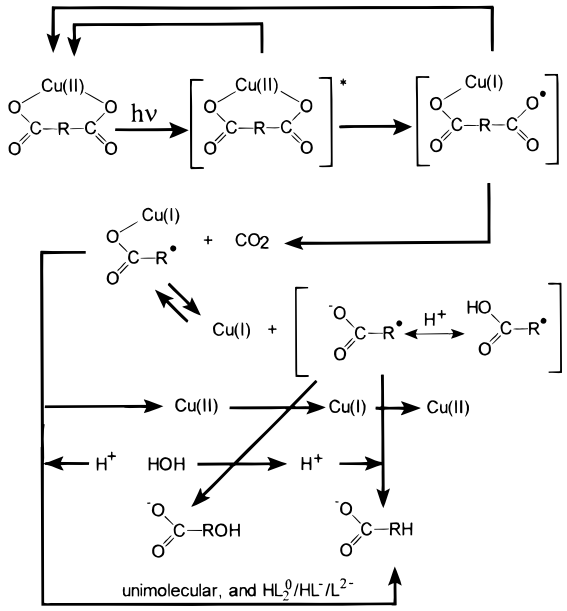

Figure 3. Reaction scheme for the photoreaction of Cu(II)/dicarboxylate complexes.

pathway of the ith Cu(II) species $Cu(II)_i$ (e.g., CuL, CuL_2, Cu(HL), etc.), the rate constants are represented as j_{i1}, k_{i2}, k_{i3}, and k_{i4}, $^{\cdot}RC(O)O^-$ represents the carbon-centered radical, Q represents any possible quenchers of $[Cu(I)\text{-}^{\cdot}RC(O)O^-]_i$ (including uncomplexed dicarboxylate species H_2L, HL^-, or L^{2-}). When the unimolecular back electron transfer of $[Cu(I)\text{-}^{\cdot}RC(O)O^-]_i$ occurs (by which the released Cu(II) immediately reforms the original complex $Cu(II)_i$ in the presence of excess ligand), Q may be a solvent molecule or may not be present. $HRC(O)O^-$ and $R(OH)C(O)O^-$ represent photoproducts (e.g., acetate and hydroxyacetate from Cu(II)/malonate system, respectively).

The stability of the carbon-centered radical influences the rate of decarboxylation to form the carbon-centered radical (relative to j_{i1}), which in turn influences the Cu(I) quantum yield in the system previously studied.[16] Once formed, the radical species $Cu(I)\text{-}^{\cdot}RC(O)O^-$ can dissociate into Cu(I) and the free carbon-centered radical $^{\cdot}RC(O)O^-$, whereby the radical (protonated and deprotonated forms) can reoxidize Cu(I) to Cu(II) or reduce another Cu(II) species to Cu(I). The latter reaction is favored by the ratio of Cu(II) to Cu(I) concentrations; competition between Cu(I) and Cu(II) for $^{\cdot}RC(O)O^-$ determines the yield of Cu(I). In the system studied as shown in Figure 3, aqueous Cu(II) species, namely, Cu^{2+}, CuL, and CuL_2 etc., are likely to be the major scavengers of the carbon-centered radical. For the Cu(II)/malonate system ($R = CH_2$), both $CH_3C(O)O^-$ and $CH_2(OH)C(O)O^-$ were formed during illumination (313 nm) of the Cu(II)/malonate complexes ($[Cu(II)]_T = 50$ μM, pH = 7.00, $[L]_T = 800$, 1700 μM), which is consistent with previous findings at 254 nm and confirmed the indirect photochemical pathway.[17]

For most Cu(II) complex systems, the decay of the intermediate $[Cu(I)\text{-}^{\cdot}RC(O)O^-]$ is unimolecular or pseudo-first order. However, in some cases (specifically with Cu(II)/malonate), the quenching effect on the photoformation of Cu(I) of free uncomplexed ligand species (which vary in concentration depending on the reaction conditions) may be considered explicitly. Therefore eq 5 can be clearly expressed as the following process:

$$[Cu(I)\text{-}^{\cdot}RC(O)O^-]_{cage} + HL^-/H_2L \longrightarrow Cu(II)\text{-}L + HRC(O)O^- \quad (7)$$

Data Analysis for Copper(I) Quantum Yields. Following the total initial Cu(I) photoproduction rate is the sum of the initial photoreaction rates of individual Cu(II) species, quantum yields ($\Phi_{Cu(I),i}$, mole $einstein^{-1}$) for individual species of the

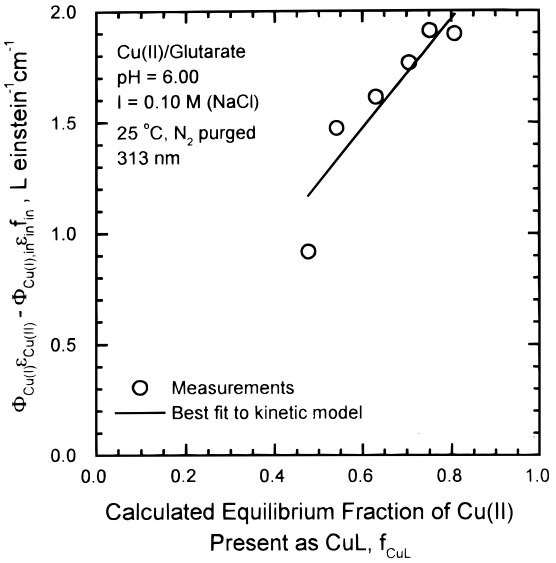

Figure 4. Comparison of measured and calculated photochemical parameters for Cu(II)/glutarate. Best fit values (multivariate linear regression) were determined from eq 8.

different Cu(II)/dicarboxylate complexes can be determined by

$$\Phi_{Cu(I)}\epsilon_{Cu(II)} = \sum_i(\Phi_{Cu(I),i}\,\epsilon_i f_i) \qquad (8)$$

where $\Phi_{Cu(I)}\epsilon_{Cu(II)}$ is an observed quantity, and the species-specific quantity, $\Phi_{Cu(I),i}$, includes $\Phi_{Cu(I),CuL}$ for CuL, $\Phi_{Cu(I),CuL2}$ for CuL_2, $\Phi_{Cu(I),Cu(HL)}$ for Cu(HL), and $\Phi_{Cu(I),in}$ for the average (mean) of all inorganic Cu(II) species.[30] Equation 8 indicates that the observed value, $\Phi_{Cu(I)}\epsilon_{Cu(II)}$ is a linear combination of the weighted value of $\Phi_{Cu(I),i}\epsilon_i$. Therefore, the fundamental quantity ($\Phi_{Cu(I),i}\epsilon_i$) of individual Cu(II) complexes (e.g., CuL, CuL_2) can be determined from a multivariate linear regression of eq 8 by varying f_i. As an example, Figure 4 illustrates the quality of fit of eq 8, which was used to determine the single variable $\Phi_{Cu(I),CuL}\epsilon_{CuL}$ for the Cu(II)/glutarate system. Cu(I) quantum yields at 313 nm for CuL ($\Phi_{Cu(I),CuL}$) of the different Cu(II)/dicarboxylate complexes (except for the malonate system) were determined by these procedures and are listed in Table 3. Good agreement between calculated and measured values was obtained for Cu(II)/adipate (within 8%) and Cu(II)/pimelate (within 19%) systems.

In the Cu(II)/malonate system, the photochemical results (measured values of $\Phi_{Cu(I)}\epsilon_{Cu(II)}$ from eq 2) obtained by varying the total malonate concentration (at constant $[Cu(II)]_T$ and pH) or varying the pH (at constant $[Cu(II)]_T$ and total malonate concentration) could not be quantitatively interpreted solely based on the Cu(II) speciation. Specifically, the decrease of the determined $\Phi_{Cu(I)}\epsilon_{Cu(II)}$ values with increasing total malonate concentration was much greater than expected in eq 8, even if the Cu(I) quantum yield for CuL_2 is assumed to be zero, as shown in Figures 5 and 6. This indicates that, in addition to the Cu(II) speciation (f_i in eq 8), some other factor involving the malonate species (e.g., $H_2L/HL^-/L^{2-}$) affected the photochemistry of the Cu(II)/malonate system for the conditions studied here.

Due to reactions of the protonated malonate species (H_2L/HL^-) with the radical species [Cu(I)-·RC(O)O$^-$] formed during illumination of Cu(II)/malonate solutions, Cu(I) photoformation rates are strongly dependent upon the concentration of free uncomplexed malonate species H(malonate)$^-$ and H_2(malonate)^0. After considering the quenching effect of free uncomplexed

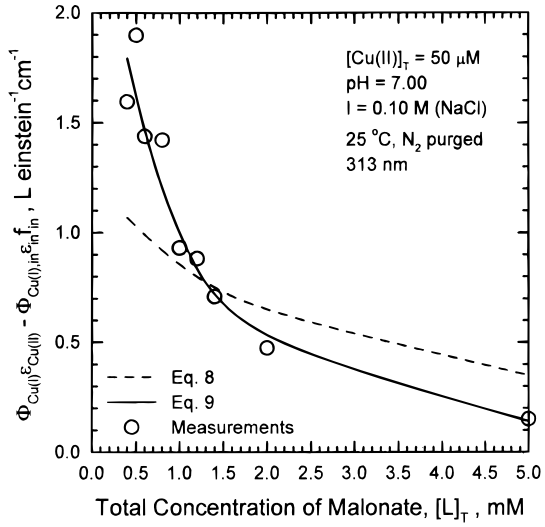

Figure 5. Comparison of measured and calculated photochemical parameters for Cu(II)/malonate as a function of total concentration of malonate. (- - -) Best fit values determined using eq 8. (—) Best fit values determined using eq 9.

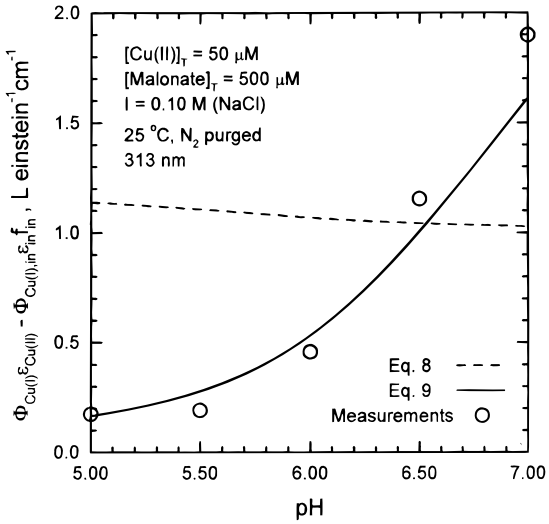

Figure 6. Comparison of measured and calculated photochemical parameters for Cu(II)/malonate as a function of pH. (- - -) Best fit values determined using eq 8. (—) Best fit values determined using eq 9.

malonate species, the quantum yields for individual species of Cu(II)/malonate can be determined from

$$\Phi_{Cu(I)}\epsilon_{Cu(II)}(1 + (k_{i3}/k_{i2})[HL^-]) = \sum_i(\Phi_{Cu(I),i}\epsilon_i f_i) \qquad (9)$$

where the values of f_i and $[HL^-]$ are determined from the equilibrium speciation calculations (Appendix I). Thus a multivariate linear regression of eq 9 (forcing the intercept through zero) is carried out to determine the coefficients $\Phi_{Cu(I),i}\epsilon_i$ (for each $Cu(II)_i$ species) and k_{i3}/k_{i2}. Values of $\Phi_{Cu(I),i}\epsilon_i$ for Cu(II)/malonate complexes determined by these procedures, and hence values of $\Phi_{Cu(I),i}$ derived therefrom, are independent of the free malonate concentration and speciation (shown in Table 3).

For the Cu(II)/malonate system, multivariate linear regression of eq 9 gave the following results (mean value ± 1 standard deviation): $\Phi_{Cu(I),CuL}\epsilon_{CuL} = 3.1 \pm 1.2$ L einstein^{-1} cm^{-1}, $\Phi_{Cu(I),CuL2}\epsilon_{CuL2} = 0.1 \pm 1.2$ L einstein^{-1} cm^{-1}, and $k_{i3}/k_{i2} = (4.7 \pm 3.0) \times 10^4$ M^{-1}. The kinetic expression (eq 9) fits the data reasonably well, as shown by the comparisons in Figures 5 and 6. As for all data, the calculated Cu(I) photoproduction

rates agree well with the measured rates (<20% difference for 16 of 17 experiments) for measured rates of Cu(I) photoproduction that varied by approximately 20-fold. Additional information about the quality of the fits is available in the Supporting Information.

Based on the values of k_{i3} (M^{-1} s^{-1}) determined using flash photolysis of Cu(II)/malonate solutions [$(7.8 \pm 1.2) \times 10^6$ for CuL, $(1.76 \pm 0.15) \times 10^7$ for CuL_2],[17] the quantity k_{i2} is calculated to be 166 ± 109 s^{-1} for the CuL pathway or 374 ± 155 s^{-1} for the CuL_2 pathway. By comparison, the first-order rate constant for unimolecular decay of an intermediate formed during flash photolysis of aqueous Cu(II)/malonate solutions was determined to be 890 ± 300 s^{-1} for the CuL_2 pathway,[17] while those for unimolecular decay of intermediates formed from the reaction of Cu^{2+} with $^{\cdot}CH_2C(O)O^-$ during pulse radiolysis of N_2O-purged aqueous Cu(II)/acetate solutions were 2.8 ± 0.3 s^{-1} for the CuL pathway and 90 ± 5 s^{-1} for the CuL_2 pathway.[34] The value k_{i2} (374 ± 155 s^{-1}) for the CuL_2 pathway determined here is in the range of reported values.

Based on the reported value of k_{i3} (7.8×10^6 M^{-1} s^{-1}) for CuL and the calculated equilibrium values of $[HL^-] = 8.4$ to 378 μM for the experimental conditions of the Cu(II)/malonate system, $k_{i3}[HL^-]$ may fall in the range from 66 to 2950 s^{-1}. Thus, the value of k_{i2} (166 ± 109 s^{-1} for the CuL pathway or 374 ± 155 s^{-1} for the CuL_2 pathway) is not greater than $k_{i3}[HL^-]$ for all of the experimental conditions studied here. This indicates the necessity to use eq 9 for the Cu(II)/malonate system, rather than eq 8 as done for other Cu(II)/dicarboxylate systems.

On the other hand, for Cu(II)/glutarate and adipate systems, eq 9 can fit the data better than eq 8, especially in the low pH ranges (pH = 4.25 to 5.75). Obviously, the two variable model is always more effective than the single parameter model from the mathematical point of view. Nevertheless, the values of $\Phi_{Cu(I),CuL}\epsilon_{CuL}$ based on eq 9 agreed within 1% of those determined from the simpler eq 8. Multivariate linear regression of eq 9 for Cu(II)/glutarate and adipate systems gave (mean value $\pm$ 1 standard deviation) $k_{i3}/k_{i2} = 39 \pm 24$ M^{-1} and 13 ± 11 M^{-1}, respectively, which are 3 orders of magnitude less than the value of Cu(II)/malonate system. Therefore, the quenching effect of free protonated ligand species in Cu(II)/glutarate and adipate systems is small. At low pH, we cannot also preclude the possibility that the formation of the CuHL species, which was not considered in these systems. Like Cu(II)/succinate system studied previously, the quantum yields of Cu(HL) species may be close to zero in Cu(II)/glutarate and adipate systems. As a consequence, the kinetic data alone do not allow us to distinguish unambiguously between formation of the CuHL species and the quenching effects of free protonated ligand species (HL). Both effects should be negligible at pH $\geq$ 6.

Previous flash photolysis studies of aqueous Cu(II)/malonate solutions (spanning even a wider pH range than that studied here) have found that H_2L/HL^- malonate species react with an intermediate, proposed to be [Cu(I)-$^{\cdot}RC(O)O^-$],[17,31] and accelerate the back electron transfer in Cu(I)-$^{\cdot}RC(O)O^-$ to reform Cu(II). However, in the study of the Cu(II)/succinate-malonate mixed ligand system ($[Cu(II)]_T = 50$ μM, $[Succinate]_T = 50$ mM, $[Malonate]_T = 100$ μM, pH = 5.00−6.50), free malonate species were not observed to quench the photoformation of Cu(I) from $Cu(succinate)^0$. This implies that the decay of the intermediates (Cu(I)-$^{\cdot}RC(O)O^-$) is specific and the structure of intermediates affects the ligand-to-metal charge-transfer reaction.

Sensitivity Analyses. The determination of molar absorptivities and Cu(I) quantum yields relies on knowledge of the Cu(II) speciation. Sensitivity analyses were performed to determine the effect of the uncertainty in calculated equilibrium Cu(II) speciation (i.e., f_{CuL}, f_{CuL2}, $f_{Cu(HL)}$, f_{in}, etc.), which is based on equilibrium constants and pK_a values listed in Table 2. It was found that the uncertainty in equilibrium formation constants of CuL and CuL_2 (if present) exhibited the greatest effect on the associated uncertainty in values of ϵ_i and $\Phi_{Cu(I),i}$. Hence, for each Cu(II)/dicarboxylate system, sensitivity calculations were carried out, for which the equilibrium constants for CuL (β_{CuL}) and CuL_2 (β_{CuL2}) (if present) were varied over a 4-fold range (increased or decreased by a factor of 2.0 relative to the best values of β_{CuL} and β_{CuL2} given in Table 2). For each Cu(II)/dicarboxylate system, results of these calculations (4 permutations) are summarized as ranges of the relevant parameters.

Ranges of ϵ_i (M^{-1} cm^{-1}) are: 18−21 for $Cu(malonate)^0$, 41−53 for $Cu(glutarate)^0$, 45−57 for $Cu(adipate)^0$, and 31−71 for $Cu(pimelate)^0$. Ranges of $\Phi_{Cu(I),i}$ (mole $einstein^{-1}$) are: 0.11−0.20 for $Cu(malonate)^0$, 0.05−0.06 for $Cu(glutarate)^0$, 0.04−0.05 for $Cu(adipate)^0$, and 0.04−0.06 for $Cu(pimelate)^0$. Since most of the published values of β_{CuL} and β_{CuL2} are within a factor of 2.0 of the best values cited in Table 2, the above uncertainties are considered small.

Effect of Outer-Sphere Coordination on the Cu(I) Quantum Yield. An important factor affecting the Cu(I) quantum yields for these complexes is the degree of outer-sphere coordination, as measured by the trend in equilibrium formation contants for $Cu(dicarboxylate)^0$ (β = [$Cu(dicarboxylate)^0$]/([Cu^{2+}][$dicarboxylate^{2-}$])). The $Cu(dicarboxylate)^0$ complexes studied here are 5-member to 10-member rings, which show a weakening of complexation with increasing ring size of the formed chelate.[35] Based on critical NIST evaluations for the same conditions, the following trend is observed for log (β) (25 °C, ionic strength = 0.10 M): malonate (5.04) > succinate (2.7) > glutarate (2.37) > adipate (2.3) ≈ pimelate (2.21). The constant for pimelate very likely represents the approximate minimum value due to outer-sphere complexation for these $Cu(dicarboxylate)^0$ complexes.[36] Based on this, the contribution of outer-sphere coordination in the series of $Cu(dicarboxylate)^0$ complexes are estimated ($\beta_{pimelate}/\beta_{dicarboxylate}$) to be: 0.0015 for malonate, 0.32 for succinate, 0.69 for glutarate, 0.79 for adipate, and ≈ 1 for pimelate. The systematic decrease in Cu(I) quantum yield observed for these $Cu(dicarboxylate)^0$ complexes parallels the increasing degree of outer-sphere coordination of the complexes. The presence of one or more water molecules between Cu^{2+} and $dicarboxylate^{2-}$ undoubtedly decreases the efficiency of the initial photoinduced electron transfer from $dicarboxylate^{2-}$ to coordinated Cu^{2+}. The dicarboxylate ligand structure also affects the lifetimes and rates of intramolecular electron transfer of $Cu(dicarboxylate)^0$ excited states. Any of these factors would, in turn, influence the Cu(I) quantum yield.

Photoreaction Rate Constants in Sunlight. The apparent first-order rate constants for photoproduction of Cu(I) from the Cu(II)/dicarboxylate complexes in terrestrial sunlight (solar zenith angle = 30°), $j_{i\rightarrow Cu(I)}$ (s^{-1}), are calculated to be 9.5×10^{-6} for $Cu(malonate)^0$ (assuming that the free malonate concentration is low enough to avoid any quenching effect), 7.0×10^{-6} for $Cu(glutarate)^0$, 6.8×10^{-6} for $Cu(adipate)^0$, and 6.7×10^{-6} for $Cu(pimelate)^0$. In surface seawater, a variety of reactions with photochemically produced reactive oxygen species such as superoxide ($^{\cdot}O_2^-$) and hydrogen peroxide (H_2O_2) may be involved in controlling the redox cycling of copper.[37−39] Although a recent study shows that the observed rate constants of the reactions of superoxide with Cu(I) and Cu(II) in seawater

are one order of magnitude lower than those reported in low ionic strength media,[40] comparison of the kinetic information indicates that the pseudo first-order rate constants of reactive oxygen species are at least two orders higher than those of dicarboxylate acid model ligands. This implies that reactions of Cu(II) by photochemically produced superoxide and hydrogen peroxide are likely to be the dominant sources of observed steady-state Cu(I) concentrations in sunlit surface seawater. However, the simple Cu(II)/dicarboxylate complexes studied may serve as a model of how to study the more complex natural organic compound in marine and freshwater environments.

Conclusions

The Cu(I) quantum yields of Cu(dicarboxylate)^0 follow the trend: oxalate > malonate > succinate > glutarate > adipate $\approx$ pimelate. Two important factors affecting the Cu(I) quantum yields for these complexes are relative stability of the carbon-centered radicals and degree of outer-sphere coordination, as measured by the trend in equilibrium formation contants for Cu(dicarboxylate)^0. Free uncomplexed malonate species H(malonate)$^-$ and H_2(malonate)^0 quench the photoformation of Cu(I) from Cu(malonate)^0 in a way that cannot be explained solely based on the Cu(II) speciation. Rather, a direct quenching effect must be included in order to model the observed Cu(I) photoformation successfully.

Acknowledgment. We are grateful to Professor Janet G. Hering of the California Institute of Technology for useful discussions and significant assistance with the preparation of this paper. We also thank the reviewers for valuable comments. This study was supported by the U.S. Office of Naval Research, Harbor Processes Program. A portion of this work was presented at the 217th national meeting of the American Chemical Society.

Appendix I

Extraction of Rate Constants from the Proposed Reaction Pathway of the *i*th Cu(II) Species Cu(II)$_i$. The mechanism described by eq 3−6 predicts different formation rates for CO_2 and Cu(I). The rate law for each species is

$$R_{CO_2,i}{}^0 = \Phi_{CO_2} I_a = 2.303 I_0 \Phi_{CO_2} \epsilon_{Cu(II)} [Cu(II)]_i D \equiv j_{i1}[Cu(II)]_i \quad (A1)$$

$$R_{Cu(I),i}{}^0 = \Phi_{Cu(I)} I_a = k_{i2}[Cu(I)\text{-}{}^{\cdot}RC(O)O^-]_i + k_{i4}[{}^{\cdot}RC(O)O^-][Cu(II)]_i \quad (A2)$$

$$R_{[Cu(I)-\cdot RC(O)O^-]i}{}^0 = j_{i1}[Cu(II)]_i - k_{i2}[Cu(I)\text{-}{}^{\cdot}RC(O)O^-]_i - k_{i3}[Q][Cu(I)\text{-}{}^{\cdot}RC(O)O^-]_i \quad (A3)$$

$$R_{[\cdot RC(O)O^-]}{}^0 = k_{i2}[Cu(I)\text{-}{}^{\cdot}RC(O)O^-]_i - k_{i4}[{}^{\cdot}RC(O)O^-][Cu(II)]_i \quad (A4)$$

where $R_{CO_2,i}{}^0$ is the initial rate of CO_2 production from the *i*th Cu(II)$_i$ pathway (the same as Cu(I), etc.). I_a is the total light intensity absorbed by the Cu(II)$_i$ complex being irradiated. The steady-state approximation, applied to [Cu(I)-${}^{\cdot}$RC(O)O$^-$]$_i$ and [${}^{\cdot}$RC(O)O$^-$], gives

$$[Cu(I)\text{-}{}^{\cdot}RC(O)O^-]_i = j_{i1}[Cu(II)]_i/(k_{i2} + k_{i3}[Q]) \quad (A5)$$

$$[{}^{\cdot}RC(O)O^-] = j_{i1}k_{i2}/\{k_{i4}(k_{i2} + k_{i3}[Q])\} \quad (A6)$$

The expression for the Cu(I) formation becomes

$$R_{Cu(I),i}{}^0 = \{2k_{i2}/(k_{i2} + k_{i3}[Q])\}\, j_{i1}[Cu(II)]_i \quad (A7)$$

Therefore, in the context of the simplified mechanism (eq 3−6), the relationship between the quantum yield of CO_2 and that of Cu(I) of the *i*th Cu(II)$_i$ species gives

$$\Phi_{Cu(I),i}/\Phi_{CO_2,i} = 2k_{i2}/(k_{i2} + k_{i3}[Q]) \quad (A8)$$

Appendix II

Extraction of Cu(I) Quantum Yields from the Proposed Reaction Pathway. *A. Constant k_{i3}[Q].* For most Cu(II)/dicarboxylate systems, k_{i3}[Q] is a constant (i.e., eq 5 is a unimolecular back electron-transfer reaction) or much smaller than k_{i2}. Then, $\Phi_{Cu(I),i}$ is a well-defined quantum yield. In this case, the initial rate of Cu(I) photoproduction from the *i*th Cu(II)$_i$ pathway $R_{Cu(I),i}{}^0$ in units of M/s can be expressed in terms of experimental quantities as:

$$R_{Cu(I)}{}^0 = \sum_i (R_{Cu(I),i}{}^0) = 2.303 I_0 D [Cu(II)]_T \sum_i (\Phi_{Cu(I),i} \epsilon_i f_i) \quad (A9)$$

After combining eq 2 and eq A9 we arrive at eq 8.

$$\Phi_{Cu(I)} \epsilon_{Cu(II)} = \sum_i (\Phi_{Cu(I),i} \epsilon_i f_i) \quad (8)$$

For most Cu(II)/dicarboxylate systems, the effects of the dicarboxylate concentration and speciation were interpreted solely based on their effects on Cu(II) speciation (f_i in eq 8). Thus quantum yields ($\Phi_{Cu(I),i}$) for individual species of the different Cu(II)/dicarboxylate complexes can be determined by eq 8.

B. Quenching Effect by Free Uncomplexed Malonate Species. In Cu(II)/malonate system, k_{i2} is no longer greater than k_{i3}[Q] and [Q] is the concentration of the free malonate species. In this case, $\Phi_{Cu(I),i}$ is not a constant but a function of [Q] (eq A8). For such conditions, the initial rate of Cu(I) photoproduction (M/s), $R_{Cu(I)}{}^0$, can be expressed in terms of experimental quantities as:

$$R_{Cu(I)}{}^0 = 2.303 I_0 D [Cu(II)]_T \sum_i \{2k_{i2}/(k_{i2} + k_{i3}[Q])\}(\Phi_{CO_2,i} \epsilon_i f_i) \quad (A10)$$

To keep the model as simple as possible, it is assumed that values of k_{i2} and k_{i3} are similar for each of the different Cu(II)$_i$ species undergoing photoreactions in the Cu(II)/malonate system.

Dividing eq A10 by k_{i2} and rearranging gives eq 9:

$$\Phi_{Cu(I)} \epsilon_{Cu(II)} (1 + (k_{i3}/k_{i2})[Q]) = \sum_i (\Phi_{Cu(I),i} \epsilon_i f_i) \quad (9)$$

where $\Phi_{Cu(I),i} = 2\Phi_{CO_2,i}$. For conditions of the Cu(II)/malonate photochemical experiments reported here (all data for pH $\geq$ 5.0), Q represents [HL$^-$].

Supporting Information Available: Tables containing additional information about the molar absorptivities and the photochemistry of the Cu(II)/dicarboxylate systems studied here.

This information is available free of charge via the Internet at http://pubs.acs.org.

References and Notes

(1) Sunda, W. G.; Gillespie, P. A. *J. Mar. Res.* **1979**, *37*, 761−777.
(2) Xue, H. B.; Sigg, L. *Limnol. Oceanog.* **1993**, *38*, 1200−1213.
(3) Palmer, F. B.; Butler, C. A.; Timperley, M. H.; Evans, C. W. *Environ. Toxicol. Chem.* **1998**, *17*, 1538−1545.
(4) Mills, G. L.; Hanson, A. K., Jr.; Quinn, J. G.; Lammela, W. R.; Chasteen, N. D. *Mar. Chem.* **1982**, *11*, 355−377.
(5) Sigg, L.; Sturm, M.; Kistler, D. *Limnol. Oceanogr.* **1987**, *32*, 112−130.
(6) Cabaniss, S. E.; Shuman, M. S. *Geochim. Cosmochim. Acta* **1988**, *52*, 185−193.
(7) Cabaniss, S. E.; Shuman, M. S. *Geochim. Cosmochim. Acta* **1988**, *52*, 195−200.
(8) Moffett, J. W.; Zika, R. G.; Brand, L. E. *Deep-Sea Res.* **1990**, *37*, 27−36.
(9) Xue, H. B.; Kistler, D.; Sigg, L. *Limnol. Oceanogr.* **1995**, *40*, 1142−1152.
(10) Langford, C. H.; Wingham, M.; Sarstri, V. S. *Environ. Sci. Technol.* **1973**, *7*, 820−822.
(11) Ferraudi, G.; Muralidharan, S. *Coord. Chem. Rev.* **1981**, *36*, 45−88.
(12) Hayase, K.; Zepp, R. G. *Environ. Sci. Technol.* **1991**, *25*, 1273−1279.
(13) Andrianirinaharivelo, S. L.; Bolte, M. *J. Photochem. Photobiol. A: Chem.* **1993**, *73*, 213−216.
(14) Thurman, E. M. *Organic Geochemistry of Natural Waters*; Martinus Nijhoff/Dr W. Junk: Dordrecht, The Netherlands, 1985.
(15) Buffle, J. *Complexation Reactions in Aquatic Systems: An Analytical Approach*; Ellis Horwood: Chichester, U.K., 1988.
(16) Sun, L.; Wu, C. H.; Faust, B. C. *J. Phys. Chem. A* **1998**, *102*, 8664−8672.
(17) Morimoto, J. Y.; DeGraff, B. A. *J. Phys. Chem.* **1975**, *79*, 326−331.
(18) Faust, B. C.; Allen, J. M. *J. Geophys. Res.* **1992**, *97*, 12 913−12 926.
(19) Blair, D.; Diehl, H. *Talanta* **1961**, *7*, 163−174.
(20) Moffett, J. W.; Zika, R. G.; Petasne, R. G. *Anal. Chim. Acta* **1985**, *175*, 171−179.
(21) Peterson, J. T. *Calculated Actinic Fluxes (290−700 nm) for Air Pollution Photochemistry Applications*, EPA-600/4-76-025, 1976; p 54.
(22) Faust, B. C.; Powell, K.; Rao, C. J.; Anastasio, C. *Atmos. Environ.* **1997**, *31*, 497−510.
(23) Anastasio, C.; Faust, B. C.; Allen, J. M. *J. Geophys. Res.* **1994**, *99*, 8231−8248.
(24) Westall, J. C.; Morel, F. M. M.; Hume, D. N. *Anal. Chem.* **1979**, *51*, 1792−1798.
(25) Allison, J. D.; Brown, D. S.; Novo-Gradac, K. J. *MINTEQA2/PRODEFA2, A Geochemical Assessment Model for Environmental Systems: Version 3.0 (EPA/600/3-91/021)*; U. S. Environmental Protection Agency, Athens, GA; 1991.
(26) Smith, R. M.; Martell, A. E. *Critical Stability Constants, Vols.* 1−6; Plenum: New York, 1976−1989.
(27) Smith, R. M.; Martell, A. E.; Motekaitis, R. J. *NIST Critically Selected Stability Constants of Metal Complexes Database*, Version 4.0, NIST Standard Reference Database 46, 1997.
(28) Stumm, W.; Morgan, J. J. *Aquatic Chemistry*; Wiley: New York, 1996; p 103.
(29) Caudle, M. T.; Stevens, R. D.; Crumbliss, A. L. *Inorg. Chem.* **1994**, *33*, 843−844.
(30) Faust, B. C. *Environ. Sci. Technol.* **1996**, *30*, 1919−1922.
(31) Morimoto, J. Y.; DeGraff, B. A. *J. Phys. Chem.* **1972**, *76*, 1387−1388.
(32) Das, S.; Johnson, G. R. A. *J. Chem. Soc., Faraday Trans. 1* **1980**, *76*, 1779−1789.
(33) Natarajan, P.; Ferraudi, G. *Inorg. Chem.* **1981**, *20*, 3708−3712.
(34) Freiberg, M.; Meyerstein, D. *J. Chem. Soc., Chem. Commun.* **1977**, 127−128.
(35) Coetzee, C. J. *Polyhedron* **1989**, *8*, 1239−1242.
(36) Hancock, R. D.; Martell, A. E. *Chem. Rev.* **1989**, *89*, 1875−1914.
(37) Moffett, J. W.; Zika, R. G. *Environ. Sci. Technol.* **1987**, *21*, 804−810.
(38) Micinski, E.; Ball, L. A.; Zafiriou, O. C. *J. Geophys. Res.* **1993**, *98*, 2299−2306.
(39) Voelker, B. M.; Sedlak, D. L. *Mar. Chem.* **1995**, *50*, 93−102.
(40) Zafiriou, O. C.; Voelker, B. M.; Sedlak, D. L. *J. Phys. Chem. A* **1998**, *102*, 5693−5700.